JOURNAL OF NANO- AND ELECTRONIC PHYSICS
Vol. **5** No 2, 02010(4pp) (2013)

ЖУРНАЛ НАНО- ТА ЕЛЕКТРОННОЇ ФІЗИКИ
Том **5** № 2, 02010(4cc) (2013)

Modeling and Design of AlN Based SAW Device and Effect of Reflected Bulk Acoustic Wave Generated in the Device

Saleem Khan*, Sandeep Arya, Parveen Lehana

Department of Physics and Electronics, University of Jammu, Jammu-India

(Received 15 February 2013; published online 04 May 2013)

Investigations of the effect of generation and reflection of bulk acoustic waves (BAWs) on the performance surface acoustic wave (SAW) device using finite element method (FEM) simulation is carried out. A SAW delay line structure using Aluminum Nitride (AlN) substrate is simulated. The dimension of the device is kept in the range of the 42 × 22.5 μm in order to analyze the effect in MEMS devices. The propagation of the bulk wave in all the direction of the substrate is studied and analyzed. Since BAW reflect from the bottom of the SAW device and interfere with the receiving IDTs. The output of the SAW device is greatly affected by the interference of the BAW with SAWs in the device. Thus in SAW devices, BAW needed to be considered before designing the device.

Keywords: Surface acoustic waves, MEMS, SAW device, Bulk acoustic waves, Interdigital transducer (IDT), Finite element method (FEM).

PACS numbers: 07.10.Cm, 68.35.Iv

1. INTRODUCTION

Surface acoustic wave (SAW) devices have been intensively study for past recent years due to their high performance filters with applications in communication systems (mobile phones, wireless local area networks) [1, 2]. SAW sensors demonstrate superior selectivity for the detection of chemical molecules. SAW chemical sensors are extremely reliable due to their design, compatible with modern technologies such as MIC (microwave integrated circuits), MEMS (micro-electromechanical-systems), CMOS, CCD (charge coupled devices) and integrated optic devices. Some of the unique properties of the SAW devices are the compact structure, high sensitivity, small size, outstanding stability, low cost, fast real-time response, passivity, and above all the ability to be incorporated in complex data processing systems [3-6].

Lord Rayleigh in discovered 1885 Surface acoustic waves and are often named after him as Rayleigh waves [7]. A surface acoustic wave is a type of mechanical wave motion which travels along the surface of a solid material called substrate. The amplitude of the wave decays exponentially with distance from the surface into the substrate, so that the most of the wave energy is confined to within one wavelength from the surface [8]. Acoustic waves in SAW devices are generation and received using various types of transducers such as bulk acoustic wave (BAW) transducers, shear wave transducers and interdigital transducers (IDT). IDTs are widely used transducer in SAW devices. These transducers are metal electrodes deposited over the piezoelectric substrate having shape of a comb. The basic structure of a SAW device is shown in Fig. 1.

The surface acoustic waves make use of the piezoelectricity in order to propagate. The Piezo Plane Strain application mode from MEMS module is dedicated to model the piezoelectricity and computes the global displacements (u; v) in the x and y directions and the electric potential (V) in a state of plane strain. These dependent variables represent the degrees of freedom. The piezoelectric constitutive equations give the relation between the stress, strain, electric field and electric displacement:

$$T = c_E S - e^T E$$
$$D = eS + \varepsilon_S E$$

where T represents the stress matrix, S the strain matrix, E the electric field, D the electric displacement matrix, c_E is the elasticity matrix, e^T is the piezoelectric matrix and ε^S is the permittivity matrix.

An IDT is a bidirectional transducer: it radiates energy equally on both sides of the electrodes. These IDTs are used for the conversion of electrical signal into acoustic waves and vice versa. Never the less they also introduce secondary effects such as reemission, BAW, diffraction, phase speed variations, reflections and electromagnetic coupling. These effects affect the performance of the SAW device [9]. The generation and effect of BAWs in SAW devices have been reported by some researchers [10-13]. The BAW launched from IDT transforms to shear SAW and further couples with radiating BAW and significantly affecting the admittance of the device. The net amount of the radiated BAW depends on the number of finger pairs in IDT [14].

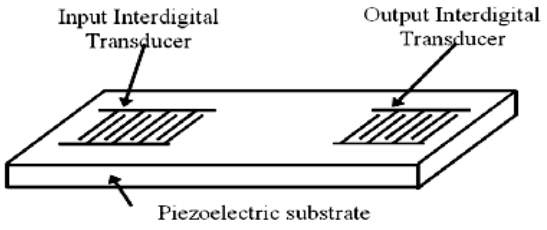

Fig. 1 – Schematic of basic SAW device

In this research work Finite Element Method (FEM) modeling of a SAW carried out and the effect of BAW radiation reflected from the bottom of AlN based SAW

* saleemqkhan@gmail.com

device is investigated caused by IDT electrodes. In the following sections theory of BAW radiation in a SAW device, methodology of work, results and discussion are presented.

2. THEORY OF BAW RADIATION IN SAW DEVICES

The explanation of generation and propagation of BAW in a SAW device with IDT transducers is well explained in [9] and [15]. BAW propagates inside the medium of substrate when the IDTs are excited in a SAW device. Fig. 2 shows the propagation of BAW takes place along with SAW at an angle of ± α symmetric about the normal to the surface in SAW devices. Condition according to which the constructive interference occurs during the propagation of BAW is given below

$$2d\sin\alpha = \lambda_B = \frac{V_B}{\lambda}$$

where λ_B the BAW wavelength and V_B speed of the bulk waves, d is the thickness of the electrodes, and λ is the wavelength of SAW. The cut off frequency f of BAW effect can be obtained from above equation by substituting the SAW synchronous frequency f_0 i.e.

$$f\frac{\sin\alpha}{V_B(\alpha)} = \frac{1}{2d} = \frac{f_0}{V_R}$$

$$\Rightarrow f > \frac{V_{B\min}}{2d}$$

Thus the minimal speed of the bulk wave (V_{Bmin}) is generally greater than the Rayleigh wave velocity (V_R). The BAW radiation power from IDT highly depends on the number of IDT finger pairs and BAW radiation becomes small for IDTs with large number of finger pairs [10].

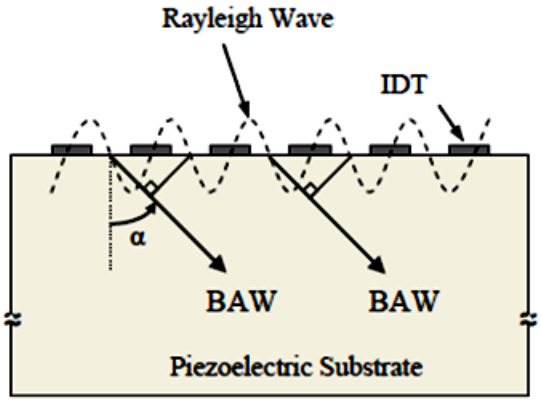

Fig. 2 – Propagation of BAW in SAW devices [13]

3. METHODOLOGY

Modeling and simulation of SAW devices had been reported by many researchers [9-14]. In the following paragraphs various parameters such as geometry, material, boundary conditions, and procedure used to perform to investigate the effect of reflected BAW in AlN based SAW delay line device is presented. The piezoelectric module and direct solvers is used to perform the simulation. AlN based SAW device with resonance frequency of 1.44 GHz is modeled. A 2D geometry of the device is shown in the Fig. 3. The device has following dimensions, the size of the substrate is 22.5 × 42 μm, transmitter and receiver IDT having dimensions of 1 × 0.1 μm, and delay line of length is 24 μm. SAW energy is confined within 1 λ wavelength thickness of substrate, and the BAW travels towards the solid core of the substrate [9]. Aluminum Nitride substrate is used as the substrate material in the simulation. The material properties such as dielectric constant, elastic constants, piezoelectric strain constant and density of the substrate are taken from [13]. The top surface of the substrate is assumed as stress free, the bottom and the side surfaces are fixed in its position, an alternating potential of 10 V is applied for the transmitting electrodes. The time domain response analysis is performed for aluminum electrode. The thickness of electrode is 0.1 μm. The displacement and potential of SAW at the receiver electrode, displacement of BAW recorded during the simulation.

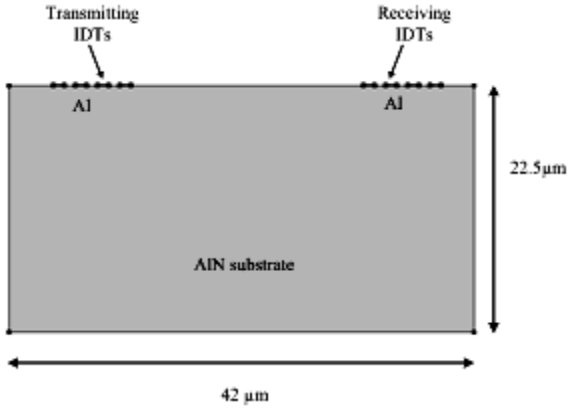

Fig. 3 – Geometry of 2D SAW device used in the simulation

4. RESULT AND DISCUSSION

The time domain analysis of the SAW device is performed for time duration of 10 ns. The total displacement of the substrate and potential is recorded at an interval of 0.2 ns during analysis. Fig. 4a to j show the surface displacement plot of generation and propagation of acoustic wave into the SAW substrate observed at time 0.2 ns, 1 ns, 2 ns, 3 ns, 4 ns, 5 ns, 6 ns, 7 ns, 8 ns, and 9 ns. SAW velocity in AlN substrate is 5740 m/s, time taken by the SAW to propagate from transmitter to the receiver is 7.2 ns. BAW is generated from the IDTs and travels in the substrate which can be clearly seen in the 2D surface plots. The values of total displacement amplitude observed at the first electrode of the receiver IDT at times 0.2 ns and 1 ns as extracted from Fig. 4a and b are 0.377×10^{-10} m and 1.044×10^{-10} m, respectively. The displacement amplitudes are purely due to BAW as they observed before SAW reaches the output IDTs. Fig. 5 shows the 1D plots of the electric potential at first input IDT and first output IDT for 8 ns duration of time. Thus the addition of BAW causes significant effect on the SAW device. Total electric energy during the study is plotted in

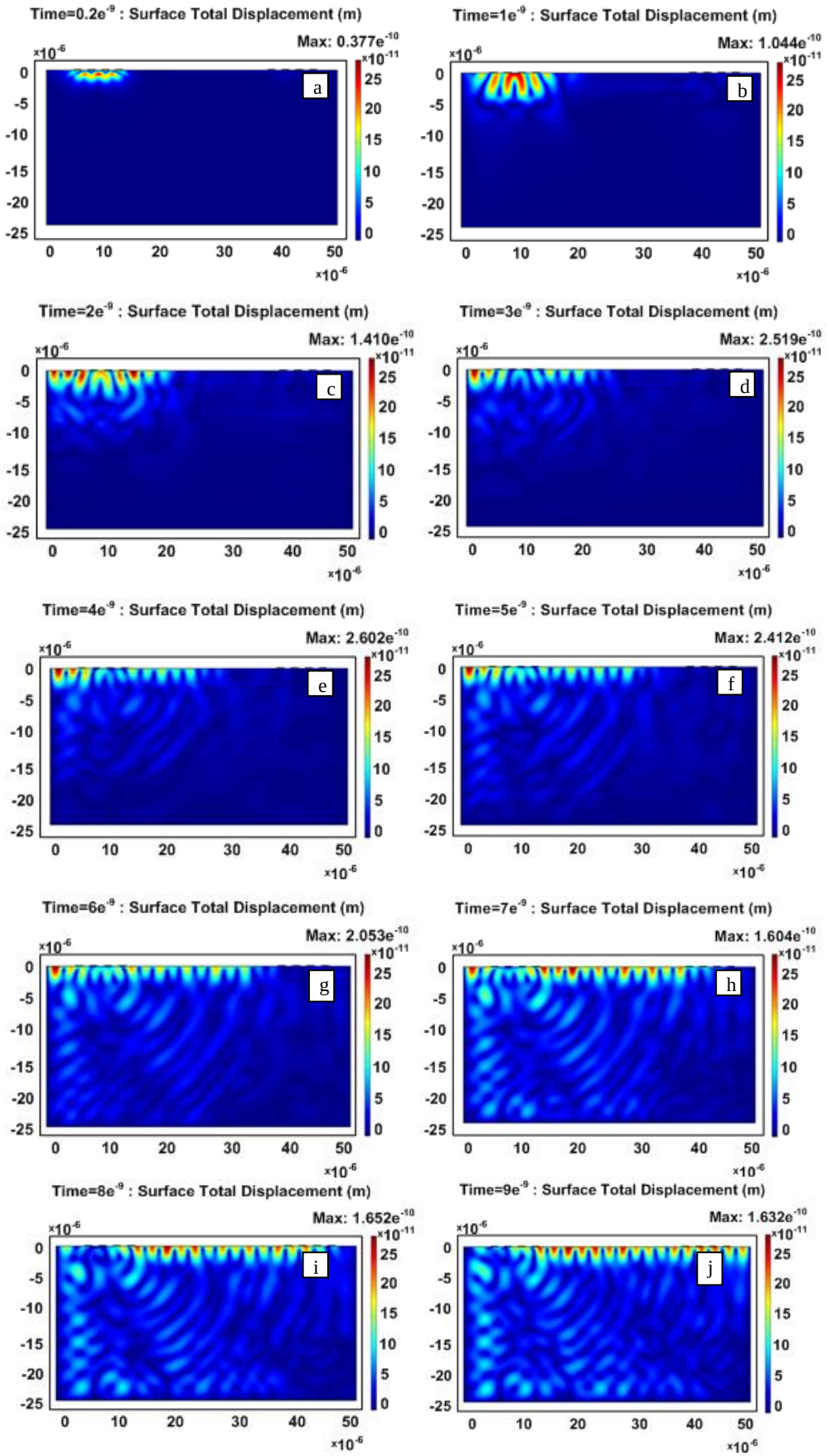

Fig. 4 – Surface displacement plots of the SAW device with IDT electrode of Al with thickness of 100 nm, showing propagation of SAWs on the surface and BAW into the interior of the substrate observed at times: a) 0.2 ns, b) 1.0 ns, c) 2.0 ns, d)3.0 ns, e) 4.0 ns, f) 5.0 ns, g) 6.0 ns, h) 7.0 ns, i) 8.0 ns and j) 9 ns

Fig. 6. It is clearly evident from the surface plots shown in Fig. 3c to j that, as time progresses, the BAW propagates in several directions into the interior of the substrate. BAW radiation after internal reflection from the substrate boundaries generates secondary waves that interfere with SAW.

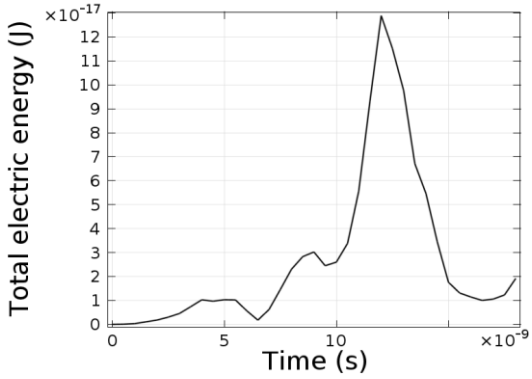

Fig. 5 – Total electric energy of the SAW device for the duration of 12 ns in time domain analysis

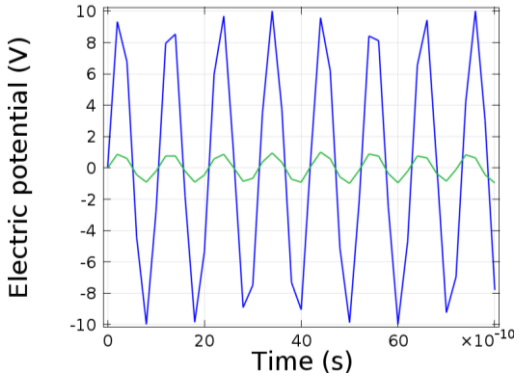

Fig. 6 – Electric potential measured at the transmitting and recieveing IDTs electrodes for 8 ns duration of the time domain analysis

The total electric energy of the SAW device is measured in the time domain analysis of the device for the duration of 12 ns shown in Fig. 5. Initially the electric energy is low and attains a value of 3×10^{-17} J at 8 ns, after reaching a value of 13×10^{-17} J at 12 ns it decreases.

The applied electric potential at the transmitting IDTs and the output electric potential measured at the receiving IDTs is plotted in the Fig. 6 for the duration of 8 ns in the time domain analysis. The blue line shows the plot for the applied sinusodial potential of 10 V and the green plot show the output potential at the receiving IDTs. In the figure it is observed that output electric potential is of low magnitude but the frequency of the signal is same i.e. no phase difference in introduced. Since the BAW reaches the receiving IDTs before SAW can reach the IDTs which interference with the SAW wave causing the amplitude difference in the input versus output signal.

5. CONCLUSION

FEM simulation of AlN based SAW delay line is performed. The investigation of the effect of BAW on the SAW device is carried out. Time domain analysis shows that BAW is generated along with the SAW from the transmitting IDTs and it propagates into the substrate in several directions. It is observed that BAW reaches at the receiver IDTs before SAW reaches. It is also observed that these waves interfere with SAW whose effect can be seen at the output signal. This investigation can be further extended to study the various parameters of the IDT affecting the performance SAW device.

REFERENCES

1. B. Zhang, E.M. Zaghloul, *53rd IEEE Int. Midwest Symposium on Circuits and Systems (MWSCAS)*, 2010.
2. T. Hoang, P. Rey, H.M. Vaudaine, P. Robert, P. Benech, *Frequency Control Symposium, IEEE Int.*, 2008.
3. C.K. Ho, E.R. Lindgren, K.S. Rawlinson, L.K. McGrath, J.L. Wright, *Sensors* **3**, 236 (2003).
4. G. Comini, G. Faglia, X. Sberveglieri, *Solid State Gas Sensing* (Springer Science Business Media LLC, New York: 2009).
5. A. Pohl, *IEEE T. Ultrason. Ferr.* **47**, 317 (2000).
6. O.K. Kannan, R. Bhalla, J.C. Kapoor, A.T. Nimal, U. Mittal, R.D.S. Yadava, *Defence Sci. J.* **54**, 309 (2004).
7. L. Rayleigh, *Proc. London Math. Soc.* **17**, 4 (1885).
8. G.W. Farnell, *Elastic Surface Waves, In Surface Wave Filters,* (Ed. H. Matthews), (John Wiley, New York: 1977).
9. D. Royer, E. Dieulesaint, *Elastic Waves in Solids II – Generation, Acoustic-optic Interaction, Applications* (Springer-Verlag, New York: 1999).
10. R.F. Milsom, N.H.C. Reilly, M. Redwood, *IEEE T. Son. Ultrason.* **24**, 147 (1977).
11. K. Honkanen, J. Koskela, V.P. Plessky, M.M. Salomaa, *IEEE Ultrasonics Symposium* **1**, 949 (Sendai: October: 1998).
12. K.J. Gamble, D.C. Malocha, *IEEE Ultrasonics Symposium* **1**, 77 (Caesars Tahoe, NV: October: 1999).
13. A.K. Namdeo, H.B. Nemade, N. Ramakrishnan, *Proc. of the COMSOL Conference* (2010).
14. K. Hashimoto, M. Yamaguchi, G. Kovacs, K.C. Wagner, W. Ruile, R. Weigel, *IEEE T. Ultrason. Ferr.* **48**, 1419 (2001).
15. M. Deng, *IEEE Ultrasonics Symposium*, 855 (2001).